Piezoresistive flexible composite for robotic tactile applications

Piezoresistive flexible composite for robotic tactile applications

Giancarlo Canavese[1], Stefano Stassi[1,2], Carmelo Fallauto[3], Simone Corbellini[3], Valentina Cauda[1], Vittorio Camarchia[1,3], Marco Pirola[3] and Candido Fabrizio Pirri[1,2]

[1]Center for Space Human Robotics@PoliTo, Istituto Italiano di Tecnologia, C.so Trento 21, 10129 Torino - Italy
[2]Department of Applied Science And Technology, Politecnico di Torino, C.so D. Abruzzi 24, 10129 Torino, Italy
[3]Department of Electronics And Telecommunications, Politecnico di Torino, C.so D. Abruzzi 24, 10129 Torino, Italy

E-mail: giancarlo.canavese@iit.it

Abstract

We present a robust and flexible tactile sensor, based on piezoresistive sensing material, having nanostructured spiky particles in a polymeric matrix, exploiting tunneling conduction mechanism when subjected to a compressive load. We have integrated here for the first time this quantum tunneling composite (QTC) with an *ad-hoc* electronic read-out circuit and a software interface to monitor and visualize the applied mechanical pressure, thus leading to a complete tactile sensor device. Concerning the sensing material, the piezoresistive composite shows an enhanced tunneling conduction, due to the presence of nickel particles with nanostructured sharp tips embedded in a silicone matrix. We registered an increase up to nine orders of magnitude of the composite electrical conduction in response to a mechanical strain. The sensor consisted in a continuous layer of functional composite sandwiched between a matrix of patterned top and bottom electrodes. The planar sensor can thus be modeled as a two-dimensional array of resistors whose value decreases by increasing the applied pressure. We also designed an *ad-hoc* electronic read-out circuit, able to read and process the resistance variations of the sensor upon a compressive load, thus providing not only the pressure intensity but also the pressure distribution data. A software interface was able to achieve the real-time tridimensional response and lead to the visualization of the compressed regions on the sensor. The present device is an efficient and low-cost prototype of tactile sensing skin, thus readily enabling its use for human robotic applications.

Keywords

Tunnelling-conduction piezoresistive composite, tactile matrix sensor, logarithmic trans-impedance amplifier, tactile imaging

1. Introduction

The fabrication of tactile sensing devices, offering the sensitivity and precision in manipulation of objects, is a key focus in research fields concerning industrial automation, service robots, and especially in space human robotics. Tactile sensing is a surface distributed function, however most of the literature refers to devices based on localized or discrete point sensing [1]. In particular, the sensing is mainly achieved upon single sensing points or discrete pads glued to a supporting surface, thus obtaining robust but locally discrete devices [2]. In contrast, only few studies deal with the whole body sensing coating, [3, 4].

Distributed tactile sensors are essential for humanoid and space service robot to obtain dynamic whole-body motion control[5]. The necessary requirements should include: (i) the complete coverage of the robot surface in order to detect collision when operating in unstructured environments[6], (ii) the high resolution and precision for the machine interaction with the external environment, (iii) the dexterous object manipulation [7, 8] and (iv) an efficient coupling to the robot surface, which can actually be accomplished with a continuous sensible layer covering the robot surface [6, 9]. Therefore, in the present work we have adopted a distributed array of sensors, being this architecture for the above mentioned requirements, the most similar to the human tactile sensing[10].

Piezoelectric [11, 12], optical[12], magnetic [13], piezoresistive [2, 14], and capacitive [15-17] principles are generally reported in the literature[18, 19] as working mechanisms for tactile sensing, thus able to transduce the strain or the induced stress, due to a tactile interaction, into an electric signal. Here we have exploited the piezoresistive working principle, since it can fulfill the requirements listed above for the distributed tactile sensing-skin when adopted for polymeric composite materials. In general, the piezoresistive sensing mechanism exploits the electric resistance variation of a conductive element upon an applied mechanical stress. In particular, recent research efforts were oriented in the preparation of piezoresistive composite materials based on insulating polymeric matrix and conductive filler particles. [9, 20, 21]. The conductive mechanism results from the compressive deformation of the polymeric matrix, reducing the distance among the conductive particles, thus building electric percolation paths and resulting in an increased electrical conduction of the overall composite [22]. The peculiarity of this solution consists in the appropriate tuning of the conductive mechanism according to the density of the particles, which are assumed to be homogeneously distributed throughout the whole polymeric matrix. In most of the studied cases [9, 23-25], the conductive particles get in physical contact with each other as soon as the mechanical load is applied [22, 26-28]. The change in resistivity is obviously a function of the filler concentration in the polymeric matrix and the percolation paths can be described by different theoretical models [29, 30]. However, most of these models fail in the behaviour prediction below the percolation threshold.

In a second type of piezoresistive composites, the conductive particles are dispersed very close to each other, but remain fully coated by a polymeric layer. Therefore, in absence of any deformation, the resistance value is infinitely high, resulting in an insulating behaviour of the composite. When a compressive load is applied, the polymeric layer between the particles decreases. Electron tunnelling then occurs, leading to percolation paths and to a large reduction of the overall electrical resistance value. During the last decade, different models were used to explain the conduction mechanism, such as the electric field induced emission [31], the Richardson-Schottky transmission types and Pole-Frenkel conduction [29]. However, the most established and wide accepted model used to predict electrical conduction in piezoresistive polymer composites is the tunnelling effect [29, 32-35].

In particular, we and other authors showed that the use of nickel filler particles with nanostructured and extremely sharp tips increases of about several orders of magnitude the composite electrical conduction in response to a mechanical strain [32, 36]. The fundamental role of piezoresistive enhancement played by the tips is inferred from the results reported by Abyaneh *et al.* [37], where silicone rubber filled with smooth zinc particle showed a considerable lower piezoresistive response at the same applied pressure. The mechanism of conduction using spiky particles results in a field assisted Fowler-Nordheim tunnelling [38]. When the composite is compressed, the probability of electrons to tunnel between neighboring particles through their sharp tips increases, leading to an exponential decrease of the electrical resistance of the sample.

The piezoresistive transduction in tactile robotic applications was for example studied by Mouri *et al.*, reporting the electric resistivity of conductive inks as function of the pressure exerted on the thin film [39], Fiorillo used metal strain gauges as branch resistances of Wheatstone bridges [40], however descrete point sensing strategy was used. Finally, Wu *et al.* measured the electrical resistance variation of a pressure sensitive graphite particles composite using a single electrode layer [41]. In another study, Yang *et al.* also used a composite conductive polymeric matrix filled with carbon powder on interdigitated electrodes [42]. However they reported a very long fabrication process and used discrete sensing nodes.

Here we report the use of a continuous and cost-effective hybrid piezoresistive materials composed by highly spiky nickel particles, showing nanostrucutred sharp tips, in a PDMS matrix.
The high mechanical flexibility, conferred by the polymer, combined with the tunability from the insulating to conductive electrical behaviour, makes this kind of composite the ideal candidate to constitute a smart sensing skin for robotic applications. In particular, our piezoresistive composite could satisfy the main requirements for an efficient tactile sensing skin, such as (i) high conformability and compliance, leading to soft materials adaptable to arbitrary curved surfaces and thus suitable for large area coverage application; (ii) broad range and high sensitivity; (iii) large area coverage; (iv) low power consumption, since the composite behaves like an insulator when no load is applied; (v) low payload; (vi) broad working temperature range, mainly depending on the polymer matrix; and (vii) insensitivity to electromagnetic external field. Moreover, due to their simple construction, generally these composites are very robust to overpressures, shocks and vibrations. Additionally, the light and flexible sensing elements based on composite polymeric material are fabricated by a cost effective process.

A part the material-related characteristics and advantages, also the electronic conditioning, data acquisition and transmission and finally information elaboration are fundamental factors for the efficient working of the overall system device. A recent survey reviews both the software and hardware issues concerning the effective use of tactile sensing signals. as well as interface electronics, communication, and processing for data interpretation[43].
The electronic signal conditioning is often embedded into the final sensor circuit (multiplexing, voltage/current control and measurement) to simplify the system routing[44]. Data acquisition and transmission, the key aspects of the entire system [45], are performed by microcontrollers and data acquisition units, in “real-time” or “quasi real-time” conditions, to assure the needed system response fastness to the external stimuli. The information is then transmitted and remotely post-processed to obtain the required pressure information, by specific algorithms implemented either on DSPs/FPGAs rather than ASIC cards, or even directly on PCs, e.g. by programs like Matlab [46]. The choice among the different solutions is driven by the system dimensions, number of samples, fast prototyping, and, above all, cost related issues.
In the present work, for the first time, a continuous and flexible film of piezoresistive composite based on tunnelling conduction mechanism is integrated with an *ad-hoc* designed electronic read-out circuit, able to read and process the resistance variations of the composite sensor upon a compressive load. In addition we developed a software interface able to achieve the real-time tridimensional graphical representation of the compressed region on the tactile device. We therefore envision efficient use of such device for the prototyping of tactile sensing skin in human robotic application as well as on human exoskeleton for motion and sensing assistance in constrictive or harsh environments.

2. Material and methods

2.1 Preparation of the sensing material

The composite was prepared using spiky nickel particles from Vale Inco (Type 123) and a Dow Corning two-component polydimethylsiloxane (PDMS, Sylgard 184) rubber. Field Emission Scanning Electron Microscopy (FESEM) images showed a nickel particle diameter range from 3,5 μm up to 7 μm with nanostructured sharp tips about hundreds of nanometers long. The metal–polymer composite samples were fabricated by dispersing the nickel powder in the PDMS copolymer at the weight ratio of 500 phr (per hundred resin). Previous works have demonstrated that this composition gives the best results in terms of sensitivity and processability of the material, since composites with higher nickel content are fragile and stiff [36, 47], whereas with lower content are obviously less sensitive. In this system the minimum amount of nickel particles in order to obtain a relevant piezoresistive response is 300 phr, with an electrical resistance variation of three orders of magnitude. Increasing the nickel content, the piezoresistive variation increases up to reach nine orders of magnitude, as shown in Fig. 3a with 500 phr [36, 48]. The blend was gently mixed in order to do not affect the electric behaviour of the composite,

thus avoiding the destruction of the tips on the particles surface. Afterwards, the curing agent was added at the weight ratio of 1:10 with respect to the PDMS copolymer and the resulting paste was outgassed for 1 hour under vacuum at room temperature. Composite curing occurred at 70 °C for 24 h.

2.2 Technological process flow

The experimental strategy adopted for the sensor matrix fabrication is based on a microcasting technique coupled with a hot embossing step where the functional material forms a continuous layer, with a constant thickness, between the patterned electrodes. In order to mould the composite materials in a controlled form, a PMMA master composed of three separated parts was fabricated by milling technique. Two planar plates where used as rigid top and bottom clamping plates, while a lateral frame was adopted to define the footprint of the sensor. Bottom and top electrodes where made of 50 μm thick polyimide film. Copper metalized polyimide samples were coated by positive photoresist and then patterned by UV lithography. Furthermore, the metal was selectively etched in Iron (III) chloride in order to use the metal pattern as electrodes. The same lithographic pattern (straight parallel strips) was used to mask both top and bottom electrodes, sandwiching the composite material, that were sealed orthogonally to each other in order to form an electrode matrix. Bottom and top electrodes were clamped between the planar plates respectively below and on the lateral frame. The hybrid structure composed of the piezoresistive composite material embedded in two polyimide films was obtained by pressing and heating the multilayer for three hours at 75 °C. The desired composite thickness (nominal thickness 0,3mm, 0,5mm and 1mm) was obtained by controlling the thickness of the lateral frame mould. Since the composite material and the electrodes layer are cured *in situ*, this approach overcomes the de-molding and the electrode adhesion problems observed with other microcasting techniques [49].

2.3 Material characterizations

Field emission scanning electron microscope (FESEM, Zeiss SupraTM 40) was employed for the morphological characterization of the nickel powder and PDMS-Ni composite.

These observations showed that the nickel powder is composed by spherical particles, in the range between 3,5 μm and 7 μm, presenting an irregular morphology (Figure 1a). The surface is indeed constituted by sharp nanometric spikes responsible for the tunnelling conduction mechanism [32, 36]. The particles have the tendency to aggregate in large clusters of several tens of micrometers, however during the mechanical mixing step with the polymer matrix, the aggregates are broken without modifying the surface morphology and consequently the conduction properties.

In the composite image (Figure 2b) the particles result well distributed and completely covered by the polymer, without touching each other. The polymeric layer between the nickel filler avoids the creation of percolation paths, thus ensuring an insulating electrical behaviour of the composite in the uncompressed state, as it will be described later.

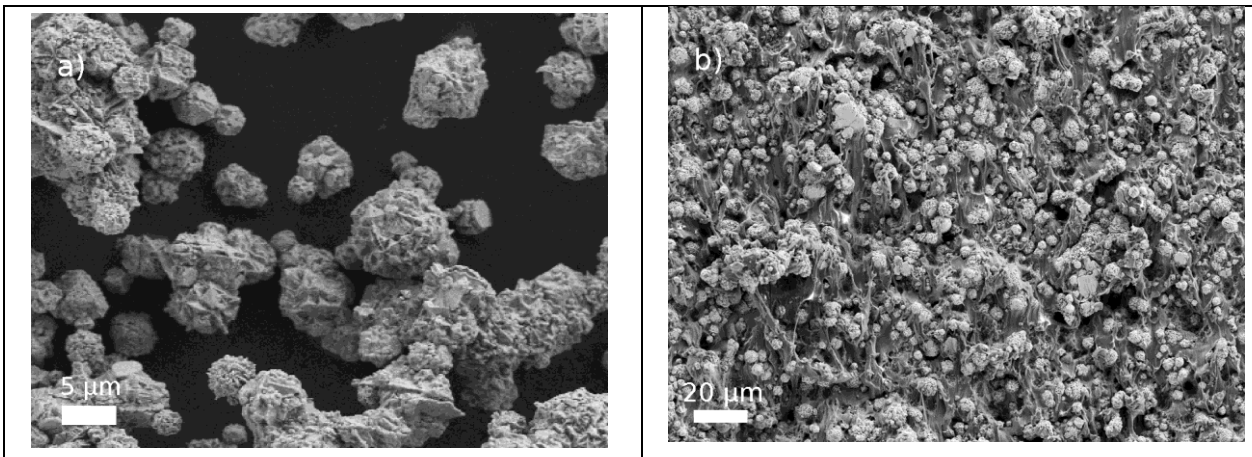

Figure 1. a) FESEM image of nickel powder; b) FESEM image of PDMS-Ni composite

The piezoresistive characterization under uniaxial compressive forces is carried out using a customized set-up constituted by a standard mechanical testing machine (MTS Qtest10) equipped with a load cell (500 N full scale) and coupled with a Keithley 2635A sourcemeter (see Figure 2). During the load/unload cycles, the voltage applied to the electrodes is kept fixed and the current is measured coupling it with the displacement and load measurements. A computer is used to acquire the measurements and synchronize all the operations performed by the whole apparatus.

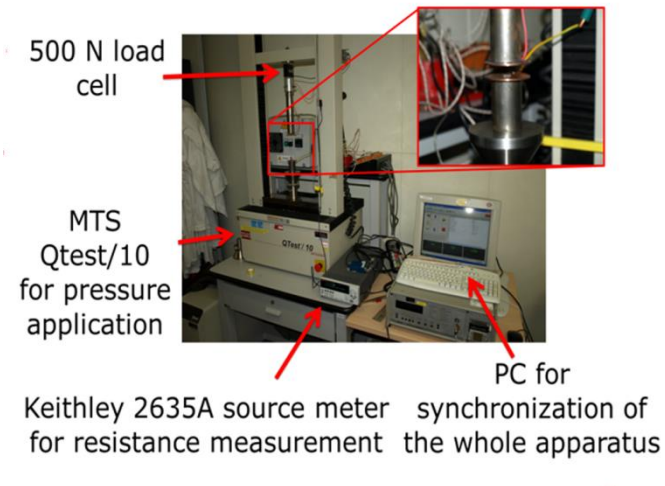

Figure 2. Image of the set-up used for the functional characterization under uniaxial compression

A plot of the functional response under uniaxial compressive pressure, measured with the set-up described above, is shown in Figure 3a. The resistance-pressure curve and the error bars were obtained by averaging over ten different measurements performed in the same conditions. The PDMS-Ni composite behaves like an insulator without any deformation (resistance approximately above 1 GΩ), whereas, thanks to the high sensitivity toward the applied stimulus, it exploits a variation of resistance up to seven orders of magnitude by increasing the pressure up to 2 MPa. The electrical resistance trends during compression and decompression cycles correspond in the range 0.8-2 MPa, taking into account the error, while there is a slight mismatch at lower pressure range. The hysteretic trend in the plot is associated to the viscoelastic nature of the PDMS that induces creep phenomena slowing the recovering of the initial sample shape and

thus the electrical resistance value. Since the hysteretic behavior is small, in this work only the compressive trend was considered for the calibration of the sensor.
The composite presented non-linear current-voltage characteristics strongly dependent on the applied pressure and voltage, as plotted in Figure 3b. As expected, by comparing the curves at different pressures under the same voltage value, the current increases with the mechanical stimulus because of the reduction of the insulator interparticles layer. At low voltage values the current follows an exponential trend typical of the tunnelling conduction phenomenon. In contrast, after a certain voltage value, the exponential growth of the current slows down up to inverting the behaviour and a negative slope is observed. This phenomenon is attributed to an accumulation of charges at the surface of the fillers, increasing the potential barrier among two nickel particles, as previously explained in details [47]. This phenomenon induces also an asymmetry in the current-voltage curve. By performing the voltage sweep from -20 V to 20 V (as in Figure 3b), the charges remain trapped in the barrier layer when the maximum negative voltage is applied at the beginning of the measurement, limiting the flowing of the current for all the negative part of the measurement till the voltage is reduced close to zero. In the positive part, the current values result higher because the flowing of the electrons is not limited till the applied voltage reaches the values needed to induce the charge accumulation. A specular behavior can be obtained performing a sweep from 20 V to -20 V [47]. However, since the resistance of our sensor is investigated at 2,5 V, this phenomenon is not a limitation for our applications.

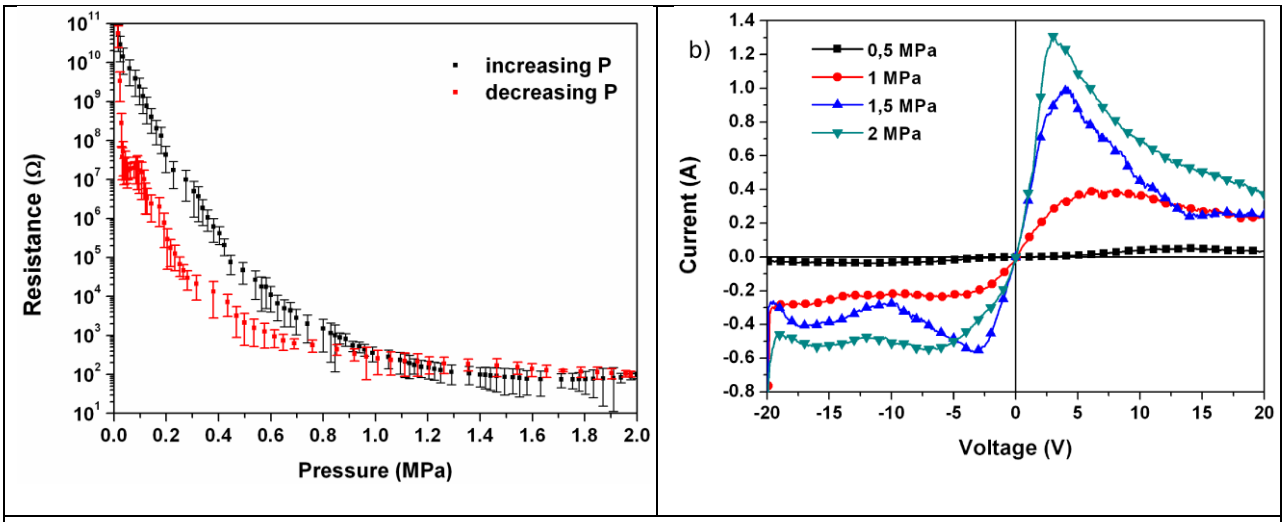

Figure 3. a) Electrical resistance and b) I-V characteristics of PDMS-Ni composite as function of uniaxial applied pressure.

To prove the device flexibility, both functional composite material and prepared sensors underwent to different bending tests. Stripe shape sample of the prepared composite with 1 and 2 mm of thickness were exposed to fatigue test using a standard test machine. The samples were subjected to a complete folding inducing a minimum bending radius of 2 mm and after 10^4 cycles no damage, crack, or permanent deformation were observed. The fabricated sensors were stressed by hand with several and heavy bending deformations and no significant variation on the piezoresistive behavior were observed. Figure 4a reports a photograph of 1mm-thick sample under bending strain after the fatigue test, showing no alteration on the sample surface. Higher degree of mechanical flexibility is shown in Figure 4b reporting a 2 mm-thick sample under a complete folding with 2 mm radius of curvature. In Figure 4c a picture of an assembled sensor bended by hand is reported.

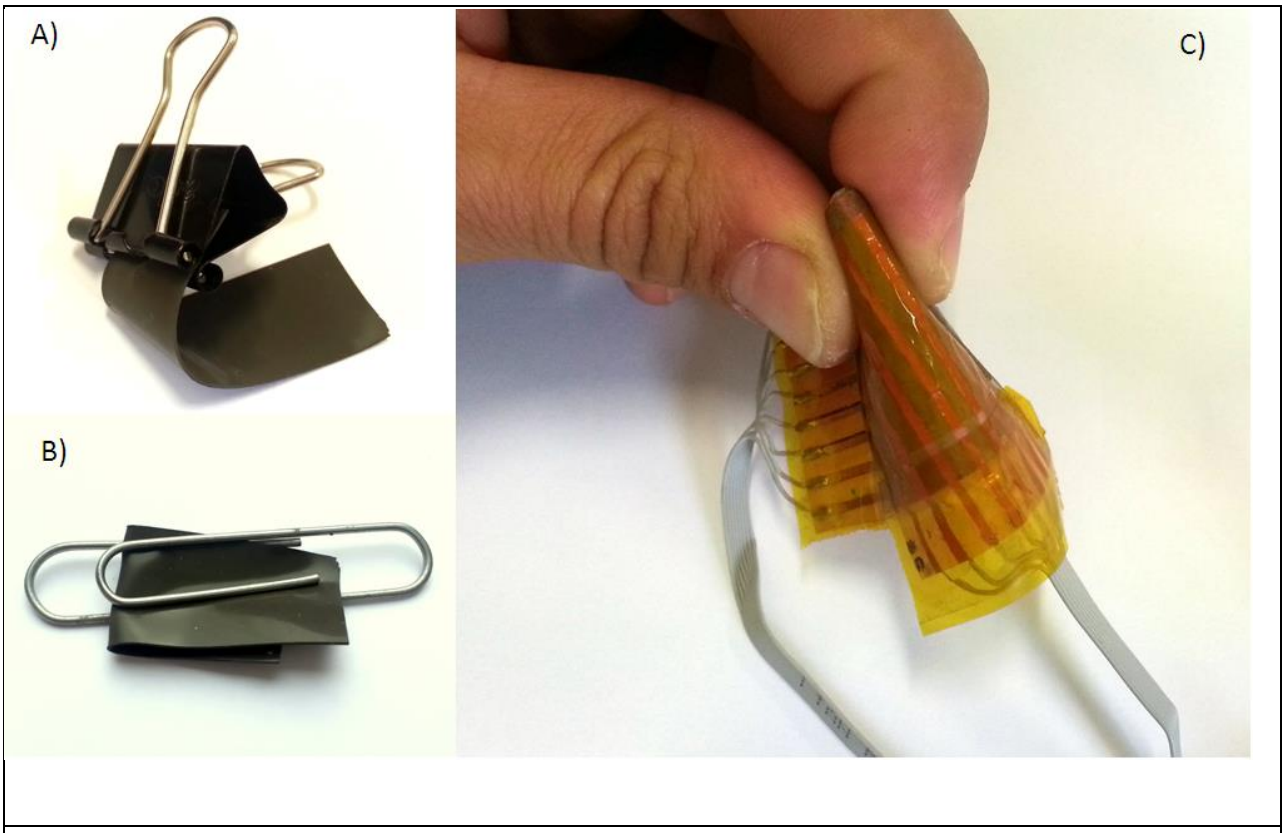

Figure 4a)…

3. Sensor design and readout circuitry

The sensor is prepared by hot embossing technique with area 40 mm x 40 mm and thickness of 1 mm. The 8x8 array pattern is fabricated by designing 8 parallel lines on two copper metalized polyimide foils used as bottom and top electrodes, respectively. The lines are 2 mm thick and the space among them is 3 mm.

The electronic board is designed to monitor the sensing material and to send the acquired data to a PC for real-time processing, thus providing the instantaneous intensity and spatial distribution of the pressure. The scheme of the architecture of the overall system is reported in Figure 5a, while Figure 5b shows a picture of the developed prototype.

The system is based on the sensing material resistance depending on the applied pressure. As described above, the electrical resistance decreases when the exerted pressure on the sample increases. According to a lumped approach, the distributed sensible area can be modeled, as a two-dimensional array of resistors whose values follow the applied pressure profile. Therefore, resistance measurements on each node of the matrix indirectly provided the pressure intensity together with its spatial distribution profile.

In the proposed system, the measure of each resistor is performed detecting the current flowing into the selected element when a known fixed voltage stimulus is provided across it.

Two analog multiplexers (ADG708 by Analog Devices) for row and column monitoring respectively are adopted to connect the observed resistor of the matrix to the measuring circuit through a low impedance path, while all others paths are kept in high impedance conditions.

For row and column scanning, the multiplexer specifics are carefully chosen to ensure that their leakage current (100 pA for the ADG708) remains negligible with respect to the expected minimum current when no pressure is exerted on the sensing pad.

Preliminary material characterizations show that the resistance of a sensor node and, as a consequence, the current to be detected has a dynamic range that can span over several decades depending on the applied pressure. For example, a typical sensor node can exhibit a resistance variation ranging from 10^2 to 10^7 ohm, and therefore, by applying a voltage stimulus of the order of 1 V, the resulting current is in the range 100 nA – 10 mA.
To tackle this huge range, an architecture based on a single temperature compensated logarithmic trans-impedance amplifier is adopted. It is worth to mention that using a single logarithmic amplifier avoided the discontinuities arising from a system with a piecewise defined gain. Moreover, notwithstanding that the current vs. pressure relationship follows an exponential behavior, the amplifier logarithmic characteristics ensuree an almost uniform uncertainty profile over the whole current range.
With respect to other proposed read-out circuits [50, 51], the proposed solution reduces to a single amplifier after the column analog multiplexer, which further helps to maintain a uniform response across the whole matrix.

The selected trans-impedance amplifier is the AD8304 (by Analog Devices).

This device allows the conversion of the current from 100 pA to 10 mA, which corresponds to a span of 8 decades, with the following conversion law (Equation 1):

$$V_{LOG} = 0.2 \log_{10} (I_{IN} /100\text{pA}) \qquad \text{(Eq. 1)}$$

In the proposed architecture, shown in the schematic of Figure 5, the stimulus is obtained by imposing a VDRIVE voltage between the row and column multiplexers. A voltage follower (implemented with the AD8629, having very low input bias current) is required at the output of the column multiplexer in order to do not compromise the measurement accuracy at low currents. A second voltage follower is used at the input of the row multiplexer to keep the stimulus constant with changes of sensing resistance of the material.
The stimulus voltage VDRIVE (1 V in this prototype) is kept constant and stable through a high precision voltage regulator (TPS7323) whose output can be regulated, to adapt the range of the resistance variation (which depends on the functional characteristics of the sensing material) to the useful range of the I-V converter.

The output voltage of the I-V range can be effectively sampled by the 12 bit analog to digital converter (ADC) embedded into the microcontroller. The microcontroller is also responsible of the continuous sequential scanning of the multiplexed channels and of the handling of the serial connection with the PC to deliver the acquired numerical data. The chip used is a PIC18F2523 manufactured by Microchip Technology. Its 12 bit ADC module has a maximum sample frequency of about 70 kHz and its Enhanced Universal Synchronous Asynchronous Receiver Transmitter (EUSART) module manages serial transmission with maximum baud rate of 115.2 kb/s. For this work the 8 bit data format, asynchronous transmission mode and a baud rate of 57.6 kb/s are selected.
The measurements on each element of the matrix sensor are carried out at a frequency of 1 kHz so that, with a 8x8 matrix, the entire planar sensor is sampled at a frequency of about 16 Hz providing true real time response and visualization.

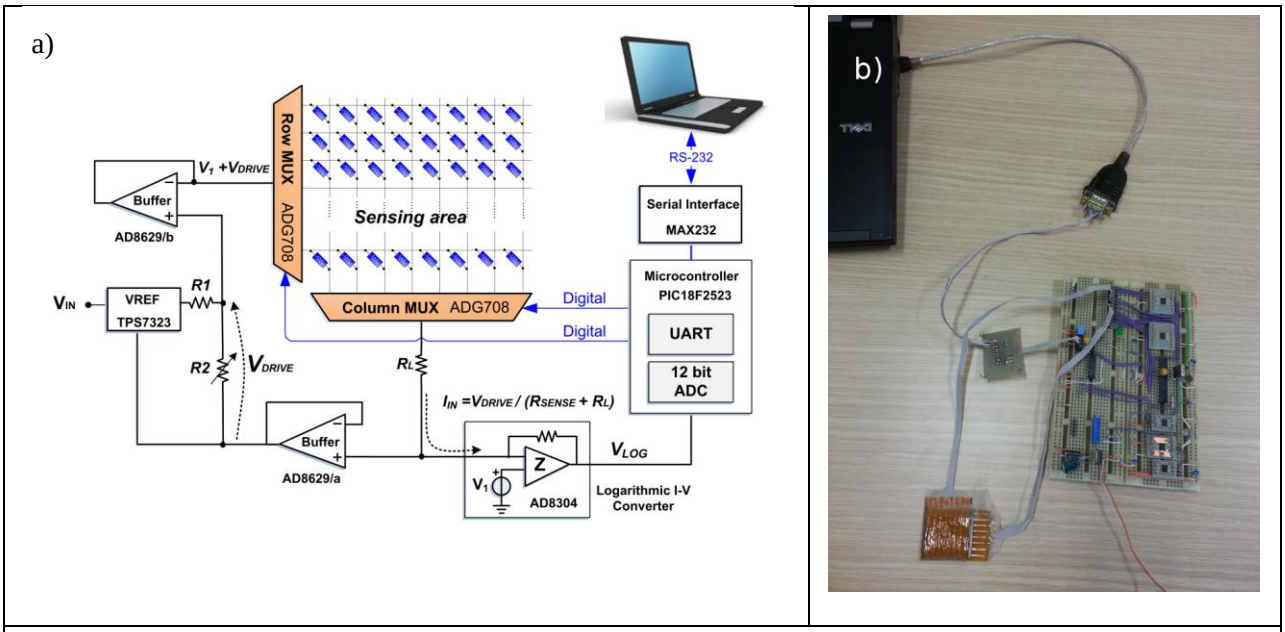

Figure 5. a) Electronic scheme of the sensor matrix read out circuit; b) Picture of the developed prototype composed by the flexible matrix sensor and the read out circuit on bread board.

The PC software program developed in Visual Basic sequentially receives from the microcontroller the pressure measurements performed on the 8x8 sensor and stores them into a measurement matrix. When the acquisition of the 64 measurements is completed, a horizontal grid, whose node heights correspond to the pressure magnitude measurements, is represented in a 3D perspective. However, in order to make the representation visually clear with smooth transactions between two adjacent nodes, the grid size is increased to a 34x34 matrix prior to plotting; a bigger display matrix is thus constructed by inserting new empty cells into the measurement matrix and by convolving the result with an isotropic progressive interpolating matrix.

The electronic system, which already exhibited interesting performance, is obtained on a 16x11 cm² laboratory developing board with through hole components. The exhibited current consumption is about 20 mA using a power voltage of 5V.

4. Device characterizations

In order to define the pressure/sensor voltage output relationship and to calibrate the electronic read out circuit, the developed device is subjected to several compressive load/unload cycles. The output of the sensor and of the reference load cell of the MTS QTest/10 are simultaneously measured and compared. The calibration law is determined by fitting the voltage output signal *S_out* of the sensor as a function of the applied compressive pressure *P* (Figure 6), obtaining (Equation 2):

$$P(kPa) = 310 * \exp(1.1 * 10^{-3} * S\_out(mV)) \quad \text{(Eq. 2)}$$

In addition, a home-made system is set up in order to investigate the response of the sensor to a variable position load and to control the mechanical cross talk effect between the adjacent nodes during the application of a dynamic (translating) load (Figure 7a). A 3-axis motorized translation stage is employed to slither a tracer point (2.5 mm of tip radius) on the sensor surface at different loads and velocities. The sensor is locked on the horizontal moving plate while the tracer point is fixed to the vertical Z axis. The planar sliding velocity of the applied compressive load is varied in the range 2.5-250 mm/s and the

pressure between 700 and 1400 kPa. The sensor is connected to the developed electronic circuit and examples of the measured and saved data of variations of electrical voltage are reported in Figure 7. In particular, the graph of the Figure 7b) shows the signals collected during the test by the eight nodes of the second line.

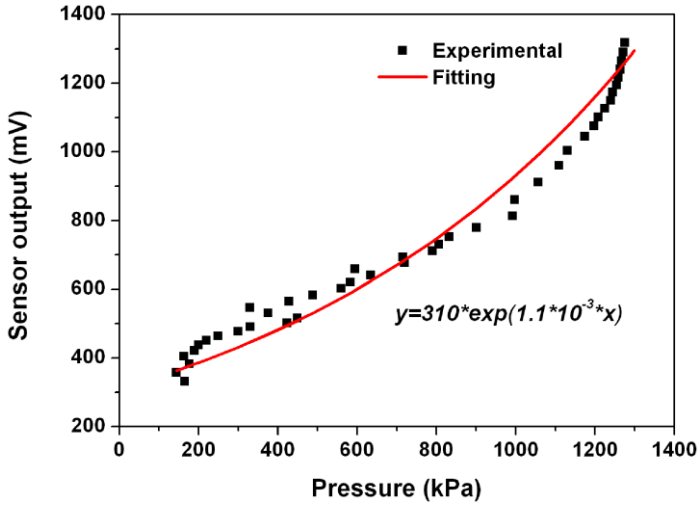

Figure 6. Experimental output of the sensor and fitting curve as a function of the applied uniaxial pressure

To verify the mechanical cross talk effect between the adjacent nodes, we applied a load that exceeds the maximum measurable pressure value in order to run the measurements with saturated signals (the curves plateau was reached at about 1.5 V) corresponding to the worse condition. In this condition the presence of cross talk phenomena should be emphasized.
The result collected using the same node line by applying 700 kPa at a sliding velocity of 250 mm/s is reported in Figure 6c. It is clear that by decreasing the applied load, the overlapping effect is drastically reduced and saturation is prevented. The graph reported in Figure 6d shows the data of round trip measurement at slow velocity (2.5 mm/s) and by decreasing the pressure load from 700 kPa to 1400 kPa. As expected the width of the saturated plateau progressively decreases and the curves assume a narrower peak shape. The different dynamic tests performed with this apparatus show a very slight amount of cross talk (signal time overlapping of two contiguous nodes), especially if we consider the relatively large size of the spherical tracer point (5 mm in diameter).

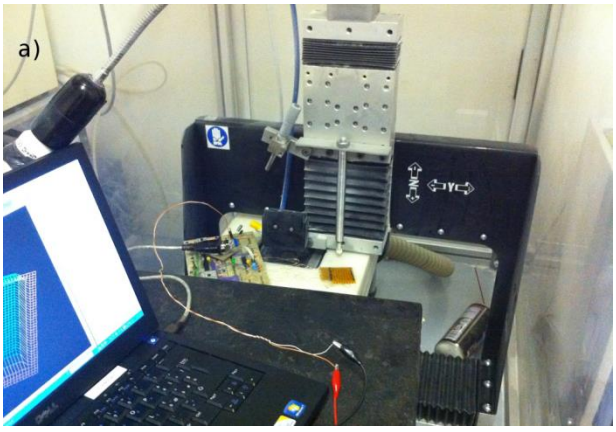

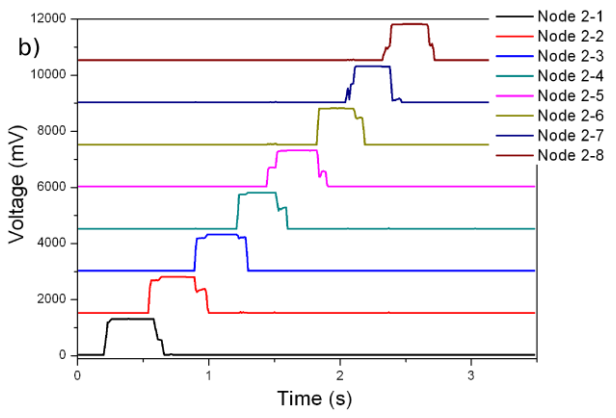

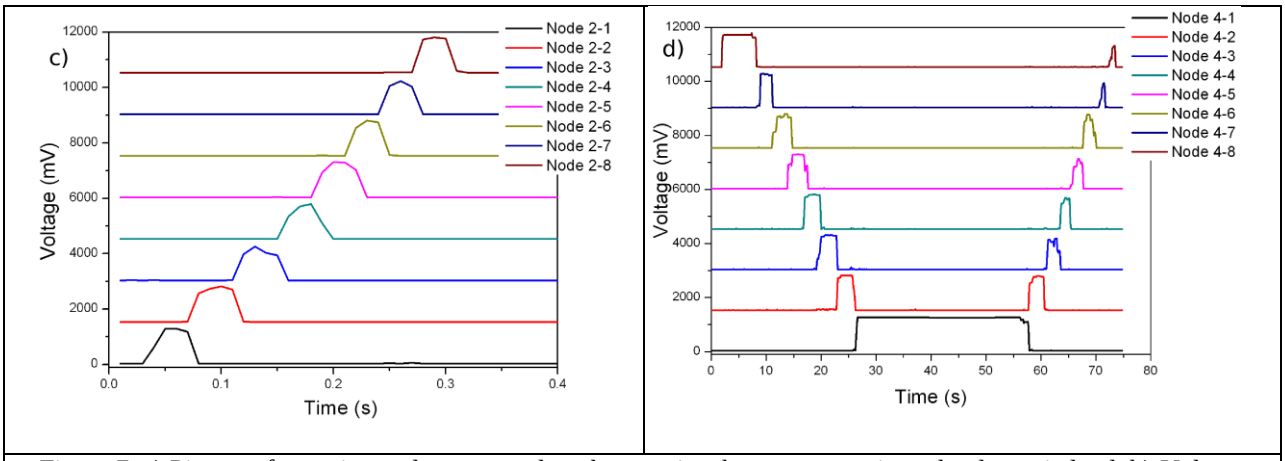

Figure 7. a) Picture of experimental set up used to characterize the sensor matrix under dynamic load; b) Voltage sensor output vs time collected from the 8 nodes of the second line during the sliding compressive load of 1400 kPa from node 1 to node 8 at 25mm/s; c)Voltage sensor output vs time collected from the 8 nodes of the second line during the sliding compressive load of 700 kPa from node 1 to node 8 at 250mm/s; d)Voltage sensor output vs time collected from the 8 nodes of the fourth line during the sliding compressive load of 700 kPa from node 8 to node 1 and back at 2,5mm/s. Each node response is shifted up of 1500 mV respect to the precedent one.

5. Final tests

After the calibration test, reported in Figure 6, the device was tested again with compressive load/unload cycles and the pressure output is compared to those registered by the load cell of the MTS QTest/10 system. The result is shown in Figure 8. The output of the sensor is almost superimposed to the real applied pressure in the range from 300 up to 900 kPa, whereas a little discrepancy is present between 900 kPa and 1150 kPa due to the saturation of the sensor output. Between 300 and 900 kPa the measurement repeatability of the single sensor is under the 10%. This figure of merit is mostly affected by the presence of hysteresis in the piezoresistive behavior. Over 1150 kPa the sensor output is saturated and measurements lack of accuracy and reliability.

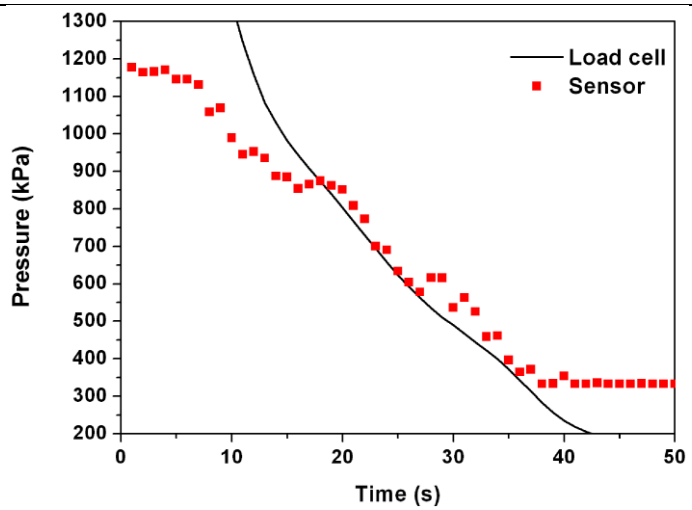

Figure 8. Comparison of the compressive strain measured with the load cell of the MTS QTest/10 and with the piezoresistive sensor.

In Figure 9 are shown two graphical results obtained with the piezoresistive sensor array and elaborated in real time by the *ad hoc* developed software. The maximum delay time of the sensor response was 50 msand it was related to the scanning approach. This fast response could be further be increased by enhancing the scanning frequency. A lateral color scale reveals the amount of compressive stress applied to the sensor, as derived from the previous calibration. Figure 8a reports a tridimensional representation of the pressure distributions measured when the sensor is subjected to a localized load applied by a pen, up to saturate the dynamics. In Figure 9b is shown the graphical representation of the footprint of a hex key pressed by fingers in two different points, which correspond to the pixels measuring a pressure above 900 kPa (see the lateral color scale).

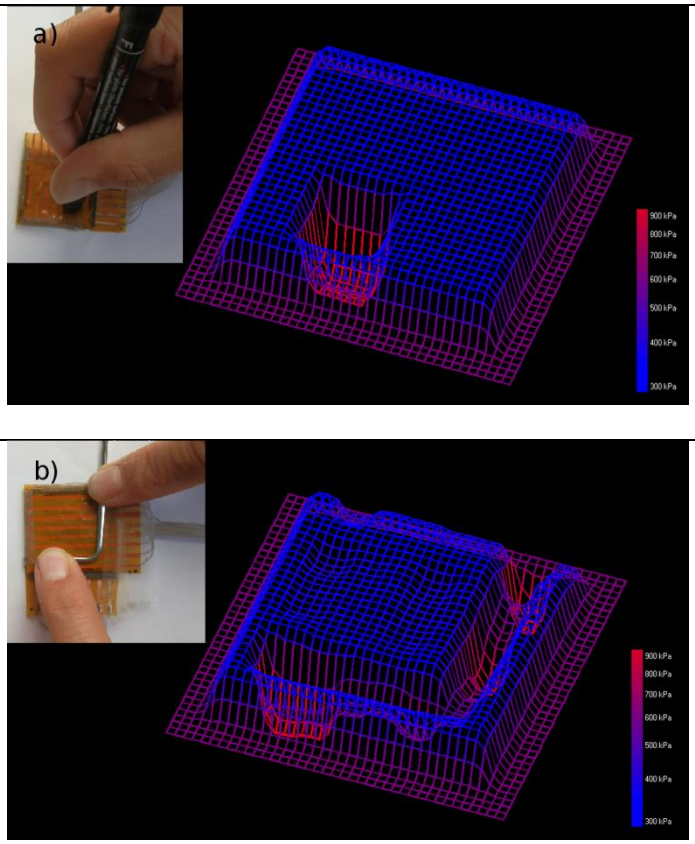

Figure 9. a) Tridimensional representation of the pressure distributions measured by the sensor matrix when it is subjected to a localized load applied with a pen until the sensor dynamic saturates and b) with a manually pressed hex key.

6. Conclusions

We have reported on the use of a piezoresistive composite as a flexible and robust tactile sensor device. In particular we have used conductive spiky nickel particles, showing nano-structured and extremely sharp tips, embedded into a silicon (PDMS) matrix. This piezoresistive composite is based on tunnelling conduction mechanism upon a mechanical compressive strain and leads to a wide variation of the electrical resistance up to twelve orders of magnitude for an applied pressure of 2 MPa.

The piezoresistive composite is prepared by microcasting and hot-embossing techniques, by sandwiching it between a matrix of patterned top and bottom electrodes. Afterwards we have integrated for the first time the piezoresistive sensor with an *ad-hoc* designed electronics read-out circuit. The electronic board is designed to monitor the sensing material, when subjected to a compressive load, and to send the acquired

data to a PC. The *ad-hoc* developed software interface is able to process the data in real-time, thus providing 3D visualization of the instantaneous intensity and spatial distribution of the pressure.
In particular the sensor device was calibrated and tests were performed to exclude the presence of mechanical cross talk effects between the adjacent nodes. Finally we have shown evidence of the correspondence between the applied mechanical pressure and the sensor output from 300 kPa up to 900 kPa, demonstrating the feasibility of a precise but simple and low-cost device.
The presented system is an efficient prototype of tactile sensing skin, it shows several interesting features, such as both space and intensity resolutions of the compressive load with a high reproducibility, high portability and ease connection to PC, as well as high flexibility, low-cost and ease manufacturing of the sensing material. Further developments will be addressed to the design of a flexible PCB based on polyimide film adopting surface mounted devices and low power-consumption processors.
Applications as a distributed tactile sensor, highly conformable to the robot surface, is straightforward, as well as its use for enhanced sensing performances in human exoskeletons.

Acknowledgements
The help of Dr. Diego Manfredi is gratefully acknowledged for the FESEM images.

References

1. M. H. Lee and H.R. Nicholls, *Review Article Tactile sensing for mechatronics--a state of the art survey.* Mechatronics, 1999. 9(1): p. 1-31.
2. K. Kim, e.a., *A silicon-based flexible tactile sensor for ubiquitous robot companion applications* Journal of Physics: Conference Series, 2006. 34: p. 399-403.
3. M. Inaba, et al., *A full-body tactile sensor suit using electrically conductive fabric and strings.* Proc. IEEE/RSJ Int. Conf. Intelligent Robots and Systems, 1996: p. 450-457.
4. Y. Ohmura, Y. Kuniyoshi, and A. Nagakubo, *Conformable and scalable tactile sensor skin for curved surfaces.* Proceeding of 2006 IEEE International Conference on Robotics and Automation. Orlando, Florida., 2006: p. 1348-1353.
5. G. Cannata, et al., *Modular skin for humanoid robot systems,* . Proceeding of 4th International Conference on Cognitive systems 2010. proceeding number 0111.
6. Bhattacharjee, T., et al. *Tactile sensing over articulated joints with stretchable sensors*. in *World Haptics Conference (WHC), 2013*. 2013.
7. Y. Kuniyoshi, et al., *Dynamic Roll-and-Rise Motion by an Adult-Size Humanoid Robot.* International Journal of Humanoid Robotics, 2004 I(3): p. 497-516.
8. V. J. Lumelsky, M.S. Shur, and Sigurd Wagner, *Sensitive skin.* IEEE SENSORS JOURNAL, 2001. 1(1): p. 41-50.
9. G. Harsaanyi, *Polymer films in sensor applications: a review of present uses and future possibilities.* Sensor Review, 2000. 20(2): p. 98-105.
10. M. Wolfe, et al., *Sensation and Perception.* , ed. Sinauer Associates Inc.2006, Sunderland, Massachusetts USA.
11. K. Takashima, e.a., *Piezoelectric properties of vinylidene fluoride oligomer for use in medical tactile sensor applications.* Sensors and Actuators A, 2008. 144: p. 90-96.
12. Dahiya, R.S., et al., *Towards Tactile Sensing System on Chip for Robotic Applications.* Sensors Journal, IEEE, 2011. 11(12): p. 3216-3226.
13. S. Takenawa, *A magnetic type tactile sensor using a two-dimensional array of inductors.* IEEE International Conference on Robotics and Automation Kobe, Japan, 2009: p. 3295-3300.

14. Lee, J.I., et al. *Development of flexible tactile sensor based on contact resistance of integrated carbon nanotubes*. in *Micro Electro Mechanical Systems (MEMS), 2013 IEEE 26th International Conference on*. 2013.
15. Wu, Z., et al., *Study of processing variables on the electrical resistivity of conductive adhesives.* International Journal of Adhesion and Adhesives, 2009. 29(5): p. 488-494.
16. M. Y. Cheng, et al., *A flexible tactile sensing array based on novel capacitance mechanism.* IEEE Transducers 2009, Denver, CO, USA, 2009: p. 2182-2185.
17. Maiolino, P., et al., *A Flexible and Robust Large Scale Capacitive Tactile System for Robots.* Sensors Journal, IEEE, 2013. 13(10): p. 3910-3917.
18. Dahiya, R.S., et al., *Tactile Sensing—From Humans to Humanoids.* Robotics, IEEE Transactions on, 2010. 26(1): p. 1-20.
19. Dahiya, R.S., M. Valle, and *Robotic Tactile Sensing: Technologies and System*, ed. Springer-Verlag2013, New York, USA.
20. Sandler, J.K.W., et al., *Ultra-low electrical percolation threshold in carbon-nanotube-epoxy composites.* Polymer, 2003. 44(19): p. 5893-5899.
21. R.H. Norman, *Conductive Rubber and Plastics* 1970, London: Elsevier.
22. X. Niu, et al., *Characterizing and patterning of pdms-based conducting composites.* Advanced Materials, 2007. 19: p. 2682-2686.
23. V. Duchaine, et al., *A Flexible Robot Skin for Safe Physical Human Robot Interaction* IEEE International Conference on Robotics and Automation Kobe, Japan., 2009: p. 3676-3681.
24. M. Shimojo, et al., *A system for simultanious measuring grasping posture and pressure distribution.* Proc. IEEE Int. Conf. Robotics and Automation, Nagoya, Japan, 1995: p. 831-836.
25. K. Weiss and H. Wörn, *The Working Principle of Resistive Tactile Sensor Cells.* Proceedings of the IEEE International Conference on Mechatronics & Automation Niagara Falls, Canada 2005: p. 471-476.
26. Q. W. Yuan, et al., *Simulations on the reinforcement of poly(dimethylsiloxane) elastomers by randomly distributed filler particles.* Journal of Polymer Science Part B: Polymer Physics, 1996. 34(9): p. 1647-1657.
27. Souza, J.F.G., R.C. Michel, and B.G. Soares, *A methodology for studying the dependence of electrical resistivity with pressure in conducting composites.* Polymer Testing, 2005. 24(8): p. 998-1004.
28. Y.J. Yang, et al., *A 32×32 temperature and tactile sensing array using PI-copper films.* Int J Adv Manuf Technol, 2010. 46: p. 945-956.
29. Strumpler, R. and J. Glatz-Reichenbach, *Conducting Polymer Composites.* Journal of Electroceramics, 1999. 3(4): p. 329-346.
30. F. Carmona, *Conducting filled polymers.* Physica A: Statistical Mechanics and its Applications, 1989. 157(1): p. 461-469.
31. L. K. H. Beek and B. I. C. F. van Pul, *Internal field emission in carbon black-loaded natural rubber vulcanizates.* Journal of Applied Polymer Science, 1962. 6(24): p. 651-655.
32. D. Bloor, et al., *A metal–polymer composite with unusual properties.* J. Phys. D: Appl. Phys., 2005. 38: p. 2851-2860.
33. F. G. Chang, et al., *Enhanced piezoresistivity in Ni–silicone rubber composites.* Chinese physics B, 2009. 18(2): p. 652-657.
34. X.W. Zhang, Z. P.Y, and X Q. Yi, *Time dependence of piezoresistance for the conductor-filled polymer composites.* J Polym Sci Part B: Polym Phys, 2000. 38(21): p. 2739-2749.
35. W. Luheng, D. Tianhuai, and W. Peng, *Influence of carbon black concentration on piezoresistivity for carbon-black-filled silicone rubber composite.* Carbon, 2009. 47(14): p. 3151-3157.
36. Canavese, G., et al., *Comprehensive characterization of large piezoresistive variation of Ni-PDMS composites.* Appl. Mech. Mater., 2012. 110-116: p. 1336 - 1344.
37. M.K. Abyaneh and S.K. Kulkarni, *Giant piezoresistive response in zinc–polydimethylsiloxane composites under uniaxial pressure.* J. Phys. D: Appl. Phys., 2008. 41: p. 135405.

38. C. J. Edgcombe and U. Valdrè, *Microscopy and computational modelling to elucidate the enhancement factor for field electron emitters.* Journal of Microscopy, 2001. 203: p. 188-194.
39. Cauda, V., et al., *Confinement in Oriented Mesopores Induces Piezoelectric Behavior of Polymeric Nanowires.* Chemistry of Materials, 2012. 24(21): p. 4215-4221.
40. Tiwana, M.I., S.J. Redmond, and N.H. Lovell, *A review of tactile sensing technologies with applications in biomedical engineering.* Sensors and Actuators A: Physical, 2012. 179(0): p. 17-31.
41. Lee, M.H., *Tactile sensing: new directions, new challenges.* International Journal of Robotics Research, 2000. 19(7): p. 636 - 43.
42. Yang, Y.J., et al., *An integrated flexible temperature and tactile sensing array using PI-copper films.* Sensors and Actuators, A: Physical, 2008. 143(1): p. 143-153.
43. Dahiya, R.S., et al., *Directions Toward Effective Utilization of Tactile Skin: A Review.* Sensors Journal, IEEE, 2013. 13(11): p. 4121-4138.
44. Koiva, R., et al. *A highly sensitive 3D-shaped tactile sensor*. in *Advanced Intelligent Mechatronics (AIM), 2013 IEEE/ASME International Conference on*. 2013.
45. Someya, T., et al., *A large-area, flexible pressure sensor matrix with organic field-effect transistors for artificial skin applications.* Proceedings of the National Academy of Sciences of the United States of America, 2004. 101(27): p. 9966-9970.
46. Alirezaei, H., A. Nagakubo, and Y. Kuniyoshi. *A highly stretchable tactile distribution sensor for smooth surfaced humanoids*. in *Humanoid Robots, 2007 7th IEEE-RAS International Conference on*. 2007.
47. Stassi, S. and G. Canavese, *Spiky nanostructured metal particles as filler of polymeric composites showing tunable electrical conductivity.* J. Polym. Sci. Pol. Phys., 2012. 50(14): p. 984-992.
48. Stassi, S., et al., *Giant Piezoresistive Variation of Metal Particles Dispersed in PDMS Matrix.* MRS Online Proceedings Library, 2011. 1299.
49. Johnson, O.K., et al., *Optimization of nickel nanocomposite for large strain sensing applications.* Sensors and Actuators A: Physical, 2011. 166(1): p. 40-47.
50. Yang, Y.J., et al., *An integrated flexible temperature and tactile sensing array using PI-copper films.* Sensors and Actuators A: Physical, 2008. 143(1): p. 143-153.
51. Vidal-Verdu, F., et al. *Large area smart tactile sensor for rescue robot*. in *Robotic and Sensors Environments, 2009. ROSE 2009. IEEE International Workshop on*. 2009.